Bioorganic & Medicinal Chemistry 20 (2012) 2930–2939

Contents lists available at SciVerse ScienceDirect

Bioorganic & Medicinal Chemistry

journal homepage: www.elsevier.com/locate/bmc

Identification of novel isocytosine derivatives as xanthine oxidase inhibitors from a set of virtual screening hits

Chandrika B-Rao [a,*], Asha Kulkarni-Almeida [b], Kamlesh V. Katkar [b], Smriti Khanna [a], Usha Ghosh [c], Ashish Keche [c], Pranay Shah [c], Ankita Srivastava [b], Vaidehi Korde [a], Kumar V.S. Nemmani [d], Nitin J. Deshmukh [d], Amol Dixit [d], Manoja K. Brahma [d], Umakant Bahirat [d], Lalit Doshi [d], Rajiv Sharma [c], H. Sivaramakrishnan [c]

[a] Discovery Informatics, Piramal Healthcare Limited, Goregaon (E), Mumbai 400 063, Maharashtra, India
[b] Department of High Throughput Screening and Biotechnology, Piramal Healthcare Limited, Goregaon (E), Mumbai 400 063, Maharashtra, India
[c] Department of Medicinal Chemistry, Piramal Healthcare Limited, Goregaon (E), Mumbai 400 063, Maharashtra, India
[d] Department of Pharmacology, Piramal Healthcare Limited, Goregaon (E), Mumbai 400 063, Maharashtra, India

ARTICLE INFO

Article history:
Received 6 January 2012
Revised 6 March 2012
Accepted 6 March 2012
Available online 14 March 2012

Keywords:
Xanthine oxidase inhibitors
Isocytosine
Virtual screening
Docking
Hit identification

ABSTRACT

In recent years, xanthine oxidase has emerged as an important target not only for gout but also for cardiovascular and metabolic disorders involving hyperuricemia. Contrary to popular belief, recent clinical trials with uricosurics have demonstrated that enhanced excretion of uric acid is, by itself, not adequate to treat hyperuricemia; simultaneous inhibition of production of uric acid by inhibition of xanthine oxidase is also important. Virtual screening of in-house synthetic library followed by in vitro and in vivo testing led to the identification of a novel scaffold for xanthine oxidase inhibition. In vitro activity results corroborated the results from molecular docking studies of the virtual screening hits. The isocytosine scaffold maintains key hydrogen bonding and *pi*-stacking interactions in the deep end of the xanthine-binding pocket, which anchors it in an appropriate pose to inhibit binding of xanthine and shows promise for further lead optimization using structure-based drug design approach.

1. Introduction

Xanthine oxidase (XO) is an important enzyme that catalyzes the transformation of physiological substrates such as hypoxanthine to xanthine and xanthine to uric acid which is excreted by kidneys. Excessive production and/or inadequate excretion of uric acid results in hyperuricemia. Hyperuricemia is associated with conditions like gout, cardiovascular mortality and metabolic syndrome including hyperinsulinemia and hypertriglyceridemia. Alleviating hyperuricemia, therefore, has therapeutic significance, and XO is a key target towards this end.[1]

Gout is a state of inflammation caused by deposition of monosodium urate crystals in joints, and is preceded by hyperuricemia.[2] Therapies include symptomatic treatments (e.g., nonsteroidal anti-inflammatory drugs, corticosteroids, IL1-traps and colchicine), and mechanism-based treatments like urate production inhibitors (XO inhibitors or XOIs, e.g., allopurinol and febuxostat) and urate excretion stimulants (e.g., probenecid).[3] Some of the small molecules currently in advanced clinical trials are topiroxostat (FYX-051, an XOI) and RDEA-594 (a URAT-1 transport inhibitor, which facilitates excretion of uric acid).[4,5] Pegloticase, a pegylated porcine urate oxidase, which mops up the excess uric acid and is effective in reversal of chronic tophaceous gout, has recently been approved by US FDA for advanced cases of treatment-resistant gout.[4,6]

It is commonly believed that 90% of the cases of hyperuricemia are due to under-excretion rather than overproduction of uric acid.[7] However, recent clinical trials of RDEA-594 demonstrated that stimulation of uric acid excretion was successful in reducing uric acid levels in only about 67% of the patients, while combination therapy with an XOI (allopurinol or febuxostat) could give up to 100% response in patients.[8] Thus, XOIs continue to be important for treatment of hyperuricemia.

All the currently available treatments come with their own sets of adverse effects. A common side-effect of all cause-based treatments (XOIs and uric acid excretion stimulants) seems to be an increase in the occurrence of gout flares in the early stages of treatment, which usually subside as the uric acid levels in the body decrease. Although allopurinol has been widely used all over the world for over 50 years, in about 5% of the cases, it is associated with hypersensitivity reactions which have sometimes even been

Abbreviations: XO, xanthine oxidase; XOI, xanthine oxidase inhibitor; po, per oral; ip, intraperitoneal; Mo-Pt, molybdopterin; PASS, Prediction of Activity Spectra of Substances; AUC, area under curve; XDH, xanthine dehydrogenase.

* Corresponding author. Tel.: +91 22 30818714; fax: +91 22 30818036.
E-mail address: chandrika.rao@piramal.com (Chandrika B-Rao).

0968-0896/$ - see front matter © 2012 Elsevier Ltd. All rights reserved.
http://dx.doi.org/10.1016/j.bmc.2012.03.019

fatal. Moreover, it is contraindicated in patients with renal impairment as it is metabolized by kidney and excreted by renal route.[9] Febuxostat is metabolized in the liver and may avoid the renal side effects shown by allopurinol, but a somewhat higher incidence of hepatotoxicity was observed in clinical trials.[10] With pegloticase, the main concerns identified are related to infusion reactions, cardiovascular events, allergic reactions and immunogenicity[6] and applicability to a limited patient population with severe tophacious gout. Hence the search for better drugs having fewer adverse effects continues.

Our work was focused on finding a novel class of XOIs which may avoid some of the adverse effects of drugs currently in the market. It is known that many natural product derivatives like flavonoids,[11,12] folates[13] and lithospermic acid[14] demonstrate xanthine oxidase inhibitory activity; however, none of these is potent enough to show clinical efficacy. Among the many small molecule scaffolds reported by various researchers[15] to inhibit XO are triazoles,[16,17] pyrazoles,[18,19] isoxazoles,[20] thiadiazolopyrimidinones,[21] chalcones,[22] pteridines,[23] purine derivatives,[24] salicylic acid derivatives,[25] curcumin analogs,[26] oxopropylamides[27] and dihydropyrazoles.[28]

Although allopurinol and febuxostat are both XOIs which bind to the xanthine-binding site of XO, their exact molecular mechanisms of action differ. While allopurinol acts as a substrate that is metabolized to oxypurinol by the molybdopterin (Mo-Pt) unit,[29] which further inhibits the binding of xanthine by co-ordinating with Mo-Pt, febuxostat binds tightly in the active site and blocks the binding of xanthine, without interacting with Mo-Pt.[30] Among the other known XOIs, FYX-051[31] interacts with Mo-Pt while salicylic acid,[32] lumazine,[33] piraxostat[19] and BOF-4272[34] do not (Fig. 1).

Using computational methods, we have identified a novel scaffold containing isocytosine ring as an inhibitor of XO, which has features common to both allopurinol and febuxostat. Although the substituted pyrimidine ring shows similar non-bonded interactions as purine substrates (xanthine), the mechanism of action is akin to febuxostat as our scaffold is a pure inhibitor and not a substrate-inhibitor.

2. Results

2.1. Virtual screening using Prediction of Activity Spectra of Substances (PASS)

The PASS[35] software gives prediction of potential biological activities of a compound based on a comparison of its chemical structure with a database of available structure–activity relationships of over 250,000 compounds. Virtual screening by PASS was resorted to in order to eliminate, at the outset, compounds that lack the features of known XOIs. Thirty-two compounds with probability of activity, Pa, greater than 0.3, were selected after in silico screening of 2648 compounds from in-house synthetic library using PASS, as detailed in Section 5. Twenty-one of these were also predicted for Gout Treatment with net probability of activity over inactivity, Pa–Pi, greater than 0.3, which adds to the evidence in favor of their being active.

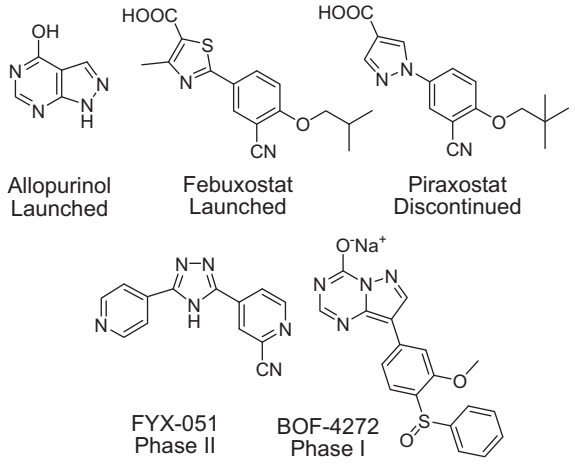

Figure 1. Structures of some important xanthine oxidase inhibitors of clinical significance.

2.2. Molecular docking studies

Twenty-four compounds (Table 1) predicted by PASS were physically available in the library. These virtual hits were docked to xanthine-binding site of xanthine dehydrogenase (XDH) co-crystallized with piraxostat (PDB code 1VDV)[19] using Glide XP docking protocol available in Schrodinger Suite of programs.[36] Glide docking scores were used to assess the docking results. Of the 24 docked compounds, 3 scored better than allopurinol (compounds **1, 2, 4**) and 3 scored within 2 kcal/mol (compounds **5**, **6**, **7**) less than allopurinol (Table 1). Based on the dock scores, only the best docked compounds were expected to show binding affinity in the in vitro assay, but all the virtual screening hits were submitted for in vitro screening as a cross-check of PASS and docking predictions.

The docked pose of compound **1** in enol form (grey) shows a good geometric fit and interactions similar to those of piraxostat with the protein (Fig. 2A). Differences were seen in the docked poses of **1, 2, 3, 4** on the one hand and **5, 6, 7** on the other (Fig. 2). Key H-bonds, *pi*-stacking interactions (face-to-face with Phe914 and face-to-edge with Phe1009) and other hydrophobic interactions found for piraxostat are maintained by **1, 2, 3** and **4** (Fig. 2A and B). Compounds **5, 6** and **7** do not have H-bonds with Thr1010 and Arg880 and either lack or have weaker *pi*-stacking interactions with Phe1009 and Phe914. Hydrophobic interactions at the mouth of the pocket with Val1011, Leu1014, Leu648, Phe649 and Phe1013 seem to be responsible for their high dock scores (Fig. 2C).

2.3. In vitro xanthine oxidase inhibition

Xanthine oxidase inhibition assay was carried out on a high-throughput system after standardization as described in the Section 5. XO was added to the test compounds or vehicle control and reaction was initiated by addition of xanthine. The UV absorbance at 310 nm, indicating the formation of uric acid was measured at 30 min at ambient temperature. The IC_{50} values were calculated for test compounds. Allopurinol was used as positive control. Three compounds, **1**, **2** and **3** exhibited xanthine oxidase inhibition in enzymatic assay. Compound **3** showed 98% inhibition at 100 μM followed by compound **2** with 79% and compound **1** with 76% inhibition (Table 1). Compounds **4, 5, 6** and **7** were inactive. In view of its good dock score, pose and interactions with protein, it was decided to test a fresh sample of **4** although it was found to be inactive.

2.4. Synthesis of compounds 1, 2, 3, 4 and confirmation of in vitro activity

Since the tested compounds were taken from a chemical library, it was necessary to synthesize them and confirm their in vitro activities. The synthesis of in vitro hits (compounds **1**, **2** and **3**) and inactive compound **4** was carried out as per Scheme 1.

The synthesized compounds were tested for xanthine oxidase inhibition using the same enzymatic assay protocol used for the library compounds. All the three active compounds showed good IC_{50} values (Fig. 3) on re-testing. Compound **3**, with an IC_{50} value of 1.4 μM, was better than allopurinol (5.7 μM) followed by **1** (9.4 μM) and **2** (30.2 μM). Although **3** was the most active com-

Table 1
Compounds screened using PASS, docked and tested in in vitro xanthine oxidase inhibition assay

Compound ID		XOI[a]		Gout treatment		Dock scores	In vitro screening
		Pa[b]	Pa–Pi[c]	Pa	Pa–Pi	kcal/mol	% inhibition (100 μM)
1	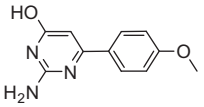	0.314	0.293	0.401	0.313	−12.6	76.25
2	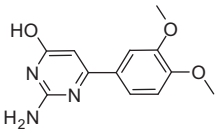	0.307	0.284	0.443	0.386	−12.99	79.63
3	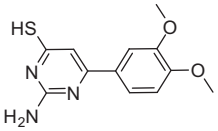	0.427	0.42	NP[d]	NP	−7.61	98.3
4	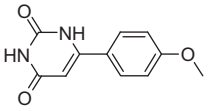	0.318	0.298	0.457	0.407	−11.06	0
5	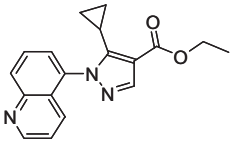	0.303	0.278	0.522	0.497	−9.58	0
6	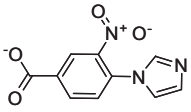	0.304	0.28	0.451	0.398	−8.94	0
7	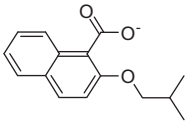	0.381	0.371	0.739	0.734	−8.82	0
8	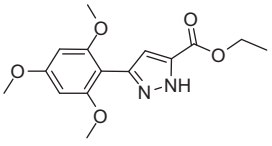	0.689	0.686	0.920	0.918	−8.32	0
9	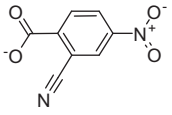	0.335	0.318	0.595	0.583	−7.57	0
10	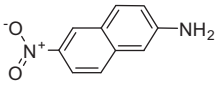	0.311	0.289	0.456	0.406	−7.39	0
11	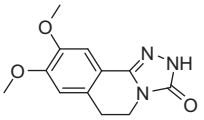	0.367	0.355	0.497	0.464	−7.36	0
12	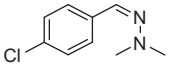	0.316	0.295	NP	NP	−7.25	0
13	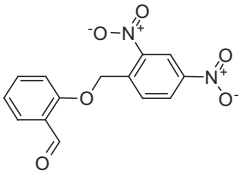	0.299	0.273	NP	NP	−7.25	0

Table 1 (*continued*)

Compound ID		XOI[a]		Gout treatment		Dock scores	In vitro screening
		Pa[b]	Pa–Pi[c]	Pa	Pa–Pi	kcal/mol	% inhibition (100 μM)
14	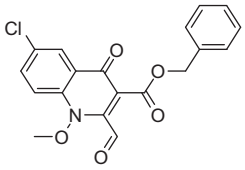	0.311	0.289	NP	NP	−7.15	0
15	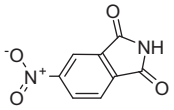	0.333	0.316	0.48	0.441	−6.97	0
16	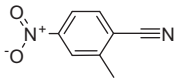	0.314	0.293	0.538	0.516	−6.85	0
17	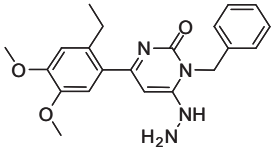	0.3	0.275	NP	NP	−6.78	0
18	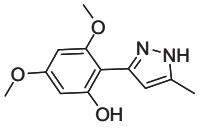	0.365	0.353	0.629	0.621	−6.74	0
19	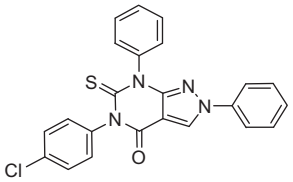	0.463	0.457	0.727	0.722	−6.62	0
20	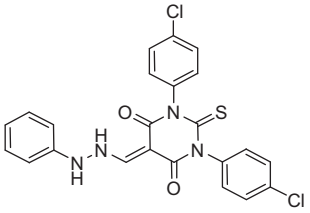	0.326	0.307	0.441	0.382	−6.48	0
21	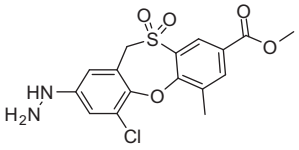	0.352	0.338	NP	NP	−5.81	0
22	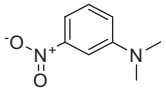	0.303	0.279	NP	NP	−5.75	0
23	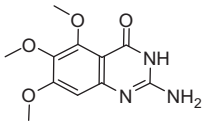	0.318	0.298	0.532	0.509	−5.14	0
24	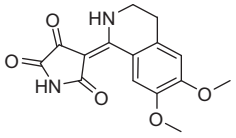	0.376	0.365	NP	NP	−4.46	0
Allopurinol[e]						−10.58	100
Febuxostat						−14.97	Not tested

[a] XOI: xanthine oxidase inhibition.
[b] Pa: probability of being active.
[c] Pi: probability of being inactive.
[d] NP: not predicted.
[e] Tested at 10 μM concentration.

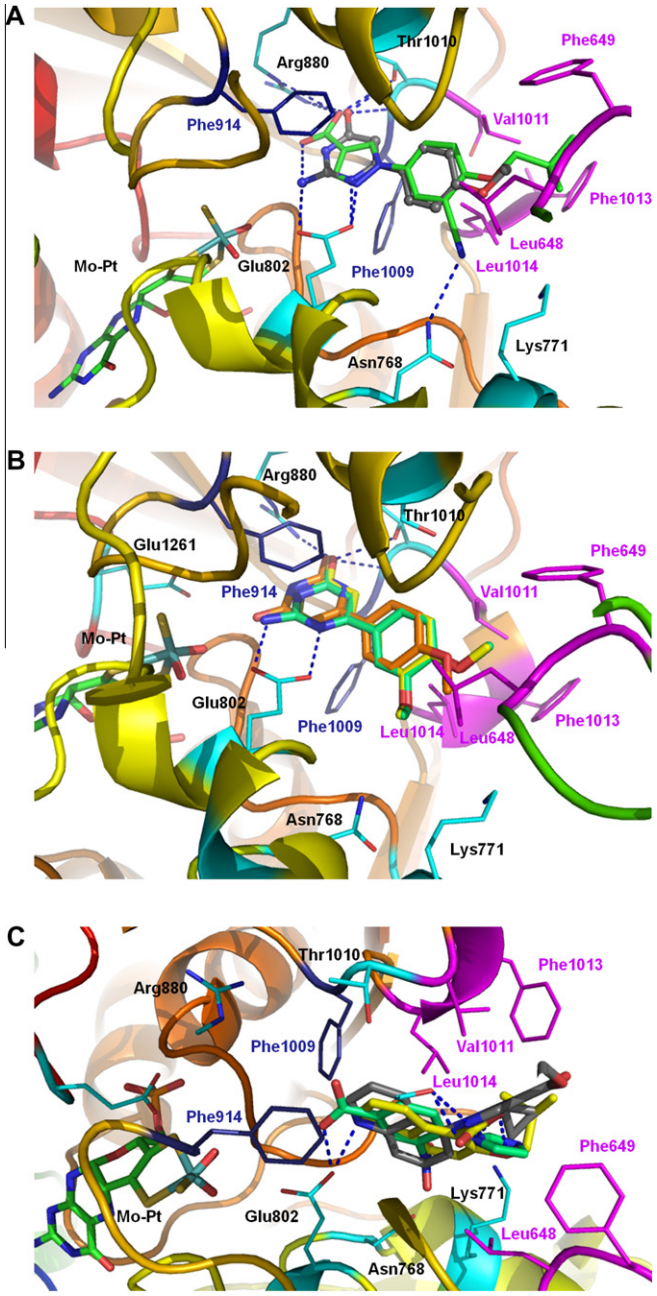

Figure 2. Docking of virtual hits in the active site of XDH. H-Bonds are depicted by blue dashed lines. Residues are colored according to the type of interaction with ligand—dark blue for *pi*-stack, magenta for other hydrophobic and cyan for polar interactions. (A) Docked pose of compound **1** (grey) and co-crystallized ligand piraxostat (lime green) show similar interactions with protein. (B) Poses of virtual hits, **2** (yellow), **3** (spring green) and **4** (brown) also show key interactions. (C) Poses of some PASS hits with good dock scores (**5** in grey, **6** in spring green and **7** in yellow) but lacking interactions at the deep end of the pocket. These figures have been generated in Pymol.[37]

pound, it was dropped due to potential toxicity issues.[38] Compounds **1** and **2** were taken forward for in vivo tests. Compound **4**, which was earlier inactive in the library screen, was again found to be inactive despite good interactions and dock score.

2.5. Effect of compounds 1 and 2 on serum uric acid in potassium oxonate-induced hyperuricemic rats

Hyperuricemia was induced by administering potassium oxonate at a dose of 250 mg/kg intraperitoneally to overnight fasted rats. Test compounds were administered 1 h later and percent reduction in serum uric acid level was computed for treated animals with respect to vehicle controls as described in Section 5. All 4 treatment groups (compounds **1, 2**, allopurinol and febuxostat) had lower serum uric acid levels than the vehicle control group (Fig. 4A). However, the percent reductions in AUC shown by compounds **1** at a dose of 100 mg/kg po and **2** at a dose of 50 mg/kg. ip (84% and 57% respectively, Fig. 4B) were less than those shown by allopurinol and febuxostat (184% and 209% respectively at 10 mg/kg po). Uric acid levels in allopurinol and febuxostat group were below basal levels, hence percent reduction was more than 100 for these compounds. These results suggested that potently active compounds could be derived by chemical modifications of compound **1** for improving enzymatic activity.

2.6. Synthesis, in vitro results and docking of compound 1 analogs

Compounds **1** and **2**, which exhibited some activity in vivo, share the same scaffold. A few analogs of **1**, varying at R1 and R2 positions (Table 2), were synthesized (Scheme 1). Methoxyphenyl pyrimidine substructure search was done on Pubchem and a few compounds (**1e, 1f, 1g**) with different substitutions at R1 and R2 on pyrimidine were purchased from commercial vendors. All these compounds failed to show in vitro enzymatic activity (Table 2). These compounds were docked to XO to find their binding modes. Most of the compounds attained very poor dock scores and did not maintain the docked pose of **1**. Removal of –OH group at R1 or its substitution with a polar group such as $–NH_2$ resulted in tremendous decrease in dock scores due to loss of H-bond interactions with either Arg880 or Thr1010 or both. Hydrophobic groups ($–CF_3$, –Cl) or bulky substituents ($–NHSO_2CH_3$, $–OCH_3$, –CN) at R1 position could not be accommodated well in the active site and the compounds adopted a flipped pose after docking. Similar flipped poses were obtained when –Cl, or $–NHNH_2$ groups were attempted at R2 position. Structure activity relationship based on this small set of molecules clearly shows that steric bulk is not tolerated at R1 and R2 positions because very little space is available at the deep end of the active site.

3. Discussion

In vitro screening of 24 virtual screening hits gave 3 active compounds, **1**, **2**, and **3**, with IC_{50} similar to or better than that of allopurinol. While compounds **1** and **2** were not predicted to be the most probable inhibitors of XO in the set of compounds assessed by PASS, they had the best dock scores. However, compound **3,** which was ranked 3rd by PASS, had a poor dock score and best in vitro activity. Its high in vitro activity could be an artifact caused by aggregation through the –SH group present in the compound.[39] Furthermore, the reactive –SH group can interact non-specifically with SH-containing compounds and proteins resulting in adverse reactions in vivo.[38] On the whole, while PASS helped in quickly identifying a set of potential actives, results of docking were much more reliable. Poorly docked compounds, with either low dock scores or poor docked poses, were found to be inactive.

Compound **4**, which attained a good dock score (−11.06 kcal/mol) and pose but turned out to be inactive in the enzymatic assay, was perhaps exceptional. It bears –OH groups at both R1 and R2 positions that can exist in tautomeric keto or enol forms. In docked pose, R2 is directed towards the oxygen atoms of Mo-Pt, and in rotated pose, R1 would face Mo-Pt. This may result in electrostatic repulsions which would prevent the molecule from adopting a pose which has pyrimidine at the deep end of the active site, but the docking program did not reflect it. It is observed that the natural substrate, hypoxanthine, flips after getting hydroxylated to

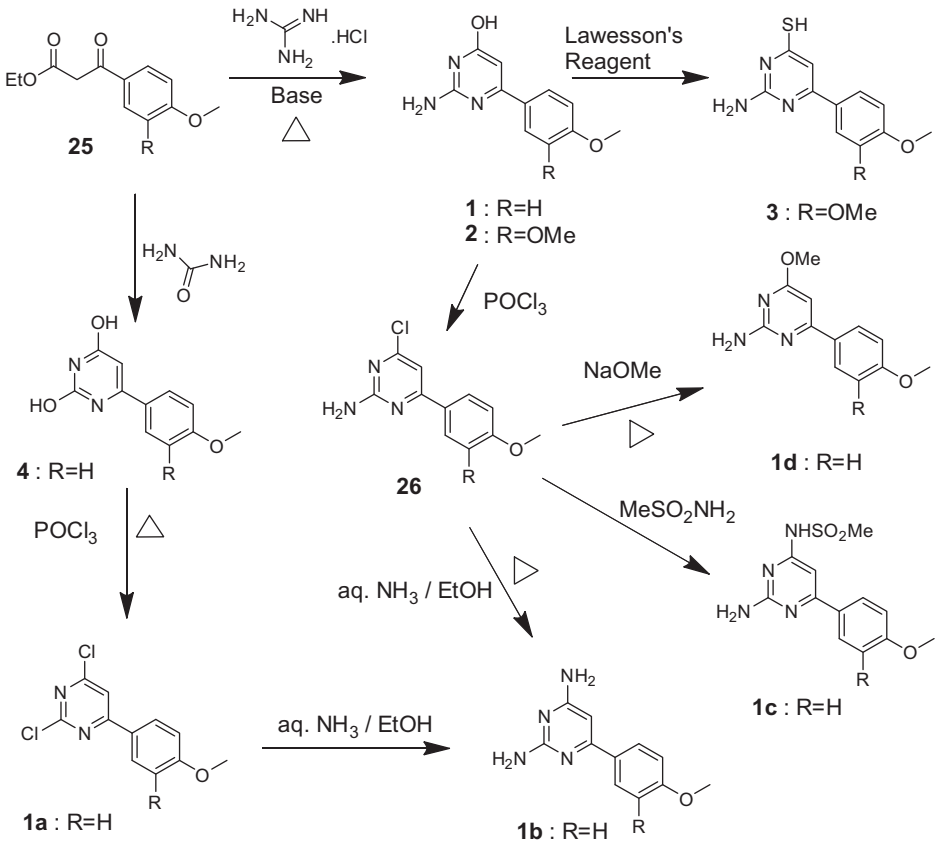

Scheme 1. Synthetic scheme for compounds **1, 2, 3, 4** (Table 1) and analogs of **1** (Table 2).

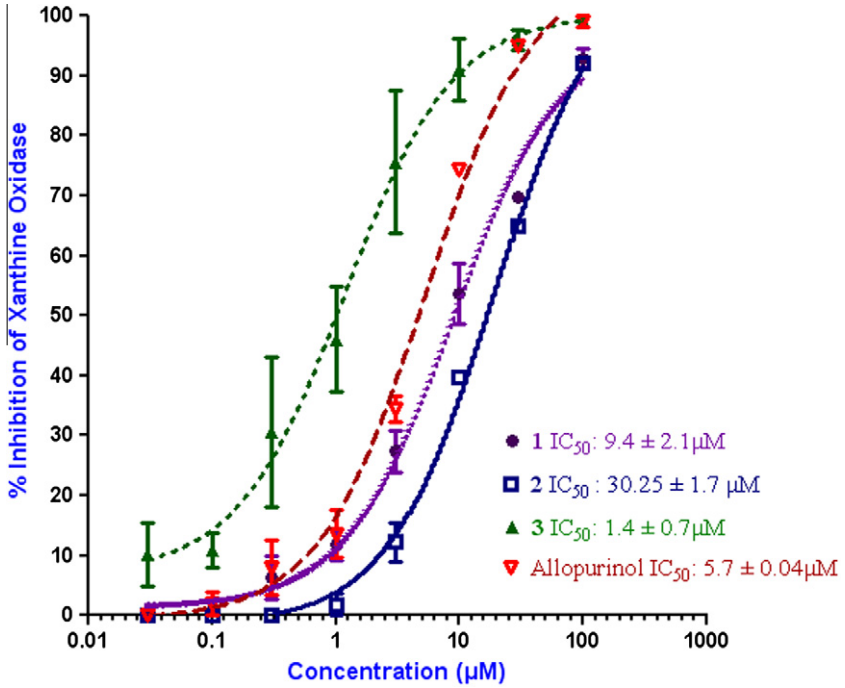

Figure 3. Dose–response curves for in vitro hits. Synthesized compounds **1**, **2** and **3** show response comparable to that of allopurinol.

xanthine and presents a different carbon atom to Mo-Pt. When this carbon also gets hydroxylated to give uric acid, the compound flips in the active site such that none of the 3 –OH groups faces Mo-Pt, and it is then ejected from the active site. The drug, allopurinol, also flips on getting hydroxylated to oxypurinol, such that both the –OH groups stay away from Mo-Pt.[29] It is also reported in

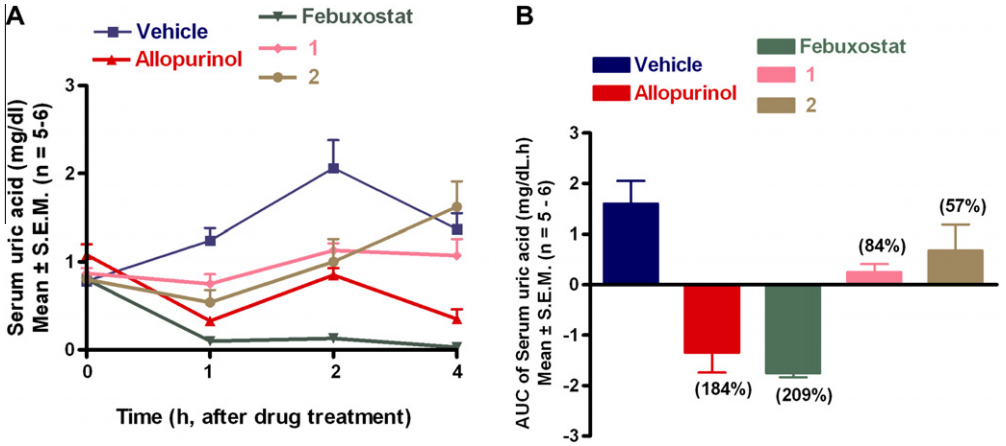

Figure 4. Antihyperuricemic effect of compounds **1**, **2**, allopurinol and febuxostat in hyperuricemic rat model. (A) Time course of serum uric acid levels for 4 h after treatment. (B) AUC of serum uric acid levels. Values in parenthesis are percent decrease in serum uric acid levels with respect to vehicle.

the literature that when dihydroxy substitution was made on purine derivatives known to be XOIs, it resulted in an inactive compound.[24] All these examples support our view that the dihydroxy compound cannot bind stably in the pose obtained by docking, and this explains why the high dock score did not translate into in vitro activity.

Further SAR at R1 and R2 positions and subsequent docking clearly show that hydrophobic and bulky substituents were not tolerated. On the whole, docking results were more reliable indicators of activity than PASS predictions. –OH group at R1 and $–NH_2$ at R2 seem to be the most appropriate choices of functional groups for this scaffold. Further improvement in the enzymatic activity may be achieved through structure-based drug design at other sites on the ligand, as outlined in section **3.1**.

In the in vivo potassium oxonate-induced hyperuricemic rat model, compounds **1** and **2** showed reduction in uric acid levels but not to the same extent as the standard compounds, allopurinol and febuxostat. Compounds **1** and **2** were also the best docked molecules with dock scores of −12.6 and −12.99 kcal/mol, better than allopurinol (−10.58 kcal/mol) but not as good as febuxostat (−14.97 kcal/mol). These results suggest that more potent enzymatic activity and better oral exposure may provide improved in vivo efficacy.

3.1. Some directions from structure-based design approach

The co-crystallized ligand, piraxostat, which is a low nanomolar inhibitor of XO (IC_{50} = 5nM), shows several interactions with the active site residues of the protein (Fig. 2A). The carboxyl group is involved in electrostatic interactions with guanidinium group of Arg880 and H-bonds to Thr1010 as well. The pyrazole ring nitrogen is involved in H-bond interaction with Glu802. Asn768 forms another crucial H-bond with the cyano group of the ligand. Besides these polar interactions, a number of hydrophobic interactions are observed as well. The pyrazole ring is *pi*-stacked between Phe914 and Phe1009. The phenyl ring has hydrophobic interactions with Leu873, Val1011 and Leu1014. The alkoxy side chain extends towards the solvent accessible region and is engaged in hydrophobic interactions with various residues at the entrance of the pocket such as Leu648, Phe649 and Phe1013.[19]

Similar interactions were observed by docking the isocytosine series of compounds. Highly polar groups such as –OH (compounds **1**, **2**) and weakly polar ones such as –SH (compound **3**) at R1 position correspond to carboxylate of piraxostat and retain H-bonds with Arg880 and Thr1010. The $–NH_2$ at R2 H-bonds to Glu802, which seems to play the role of anchoring the molecule in appropriate pose in the active site. None of the other substitutions attempted at R1 and R2 positions, be it hydrophobic or polar, showed these H-bonds, nor did they have any in vitro activity. The limited SAR at R1 and R2 positions indicates that –OH at R1 position and $–NH_2$ at R2 position are important for activity. One nitrogen of the pyrimidine ring H-bonds to Glu802, similar to pyrazole ring nitrogen in piraxostat.

Table 2
Analogs of compound **1**, synthesized or purchased and tested for in vitro activity

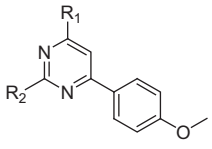

Compound ID	R1	R2	Dock scores (kcal/mol)	In vitro IC_{50} (μM)	Source
4	OH	OH	−11.06	>100	Synthesized
1a	Cl	Cl	−6.46	>100	Synthesized
1b	NH_2	NH_2	−7.87	>100	Synthesized
1c	$NHSO_2CH_3$	NH_2	−6.71	>100	Synthesized
1d	OCH_3	NH_2	−5.77	>100	Synthesized
1e	H	NH_2	−6.96	>100	Purchased
1f	CN	$NHNH_2$	−5.93	>100	Purchased
1g	CF_3	NH_2	−5.21	>100	Purchased

The mechanism of metabolism of substrate by XO requires an electrophilic carbon next to a ring nitrogen of the substrate to be positioned adjacent to Mo-Pt, with nitrogen towards Glu1261. Glu1261 acts as a general base and abstracts a proton from Mo-Pt hydroxyl group. The ionized Mo-Pt facilitates nucleophilic attack on the electrophilic carbon center. This type of motif is seen in the substrate inhibitors, allopurinol and FYX-051. Febuxostat and piraxostat do not possess this motif and do not get metabolized by Mo-Pt. Our hit has a nitrogen in the desired position, but the carbon is substituted with $–NH_2$, and is not available for attack by Mo-Pt. Hence we say that compounds **1** and **2** are pure inhibitors and not substrate inhibitors.

The terminal methoxy group exhibits weak hydrophobic interactions. Longer aliphatic chains and more hydrophobic groups could enhance these interactions and lead to further improvement in activity. Suitable groups may also be tried at *meta* position on

phenyl ring to obtain an additional H-bond with Asn768. Scaffold modifications in place of pyrimidine ring could be attempted as the nitrogen atom next to –OH group is not directly involved in any obvious interactions except possibly through water molecules, if present. Successful implementation of these modifications will be described in follow-on publications on this scaffold (in preparation).

4. Conclusions

The isocytosine scaffold has been identified from a virtual screening exercise followed by screening in uric acid production inhibition assay as a novel scaffold for xanthine oxidase inhibition. Two molecules of the scaffold exhibited in vitro xanthine oxidase inhibitory activity comparable to the standard compound allopurinol. They were tested in in vivo hyperuricemic rat model and showed reduction in uric acid levels as compared to vehicle control. Molecular docking studies of these compounds provided important insights into their binding mode and opened up the prospect of using structure-based design for improving in vitro and in vivo potency of the compounds.

5. Materials and methods

5.1. Bioactivity predictions using PASS

PASS was developed as a tool for evaluating biological activity potential of a molecule of interest.[35] Predictions are made using 2D QSAR-type models based on a large training set which includes over 250,000 substances. PASS predicts about 4000 different kinds of biological activities with a mean prediction accuracy of 85%. The list of predictable activities include main pharmacological effects (e.g., Gout Treatment, Uric Acid Excretion Stimulant), mechanisms of action (e.g. Xanthine Oxidase Inhibitor, Collagenase Inhibitor) and other effects of interest like toxicity, metabolism etc. The biological activity spectrum of the query compound is estimated from the structure–activity relationship knowledgebase (SARBase) and output in the form of probabilities of the compound being 'active' (Pa) or 'inactive' (Pi) for a biological activity. These probabilities are obtained by combining contributions made by groups of atoms in the compound, which favor or disfavor the particular activity as seen from a large structure–activity database at the backend of the software. Higher the values obtained for Pa–Pi, more the chances of the compound showing activity on a scale of 0–1. The net probability for activity of a compound can be estimated as the difference Pa–Pi. In the current study, the in silico-filtered in-house synthetic chemistry database, containing 2648 compounds which violate not more than 1 of Lipinski's Rule of 5, was screened using PASS and 646 compounds were found to have Pa–Pi >0 for Gout Treatment or Xanthine Oxidase Inhibition. Thirty-two compounds with Pa $\geqslant$ 0.3 for Xanthine Oxidase Inhibition were selected as 'hits'; all of them had Pa–Pi $\geqslant$ 0.27.

5.2. Molecular docking studies

Molecular docking studies were done using GLIDE 5.6 module of Schrodinger Suite of programs (2010).[36,40] Co-crystal structure of xanthine dehydrogenase (XDH) with piraxostat (PDB code 1VDV) was selected based on superior crystal structure parameters compared to other XO or XDH structures. No difference was seen in the xanthine binding-sites of XO and XDH crystal structures; hence we could use either of them for docking. The ligands were built within Maestro BUILD and prepared by LIGPREP module. All tautomeric forms generated at physiological pH including keto and enol forms were docked. The protein was prepared, optimized and minimized by Protein Preparation Wizard using OPLS-2005 force field. Active site for docking was defined as a grid box of dimensions $25 \times 25 \times 25$ Å^3 around the centroid of the ligand assuming that the ligands to be docked are of similar size as the co-crystallized ligand. Docking of molecules was done using Glide XP module with Epik penalties for different ionizations and tautomeric states. Ten docked poses per ligand were generated and analyzed for interpretation of final results.

5.3. Chemistry

Compounds listed in Tables 1 and 2 are either commercially available (Interbioscreen, Maybridge) or were synthesized as described in Scheme 1. All chemicals and solvents used were of reagent grade and were purified and dried by standard methods before use. All air-sensitive reactions were run under nitrogen atmosphere. All the reactions were monitored by thin layer chromatography (TLC) on pre-coated silica gel G plates at 254 nm under UV lamp using ethyl acetate/petroleum ether as eluent. Flash chromatography separations were obtained on silica gel (100–200 mesh). ^{1}H NMR spectra were recorded on Bruker Advance spectrometer (300 MHz) using tetramethylsilane as internal standard; J values are in Hertz. Chemical shifts are reported in ppm (δ) relative to the solvent peak. Mass spectra were recorded on either GCMS (focus GC with TSQ II mass analyzer and thermoelectron) with auto sampler/direct injection (EI/CI) or LCMS (APCI/ESI; Bruker daltanoics Micro TOFQ). All chromatographic purifications were done on silica gel (100–200 mesh). Melting points were measured on a MR-VIS visual melting range apparatus.

The syntheses of hits (Table 1; compounds **1**, **2** and **3**) and analogs (Table 2; **4**, **1a**, **1b**, **1c** and **1d**) were carried out as per Scheme 1 and experimental procedure below. 2-Amino-6-aryl-substituted-pyrimidin-4-ol (**1**) was prepared from corresponding ethyl-3-aryl-substituted-3-oxopropanoate (**25**) and guanidine and subsequently converted to thiol derivative (**3**) by Lawesson's reagent and to 4-chloro-6-aryl-substituted-pyrimidin-2-amine (**26**) by treatment with $POCl_3$. Compound **26** was later converted to its amine (**1b**), methanesulfonamide (**1c**) and methoxy (**1d**) derivatives by treatment with ammonia, methanesulfonamide and sodium methoxide respectively. Compound **1b** was also prepared by ammonia reaction of 2,4-dichloro-6-(4-methoxyphenyl)pyrimidine (**1a**) as shown in Scheme 1.

The structures of commercially purchased compounds (Table 2; **1e**, **1f** and **1g**) (Interbioscreen, Maybridge) were confirmed by melting point and spectral data.

5.3.1. Preparation of 2-amino-6-(4-methoxyphenyl)pyrimidin-4-ol (1)

To a stirred solution of **25** (1.0 g, 4.49 mmol) and guanidine hydrochloride (0.64 g, 6.75 mmol) in DMF (10 ml), sodium acetate (0.55 g, 6.75 mmol) was added and heated at 100 °C for 48 h. Reaction mixture was cooled to rt, diluted with water (5 ml) and pH was adjusted to 6.5. The precipitated solid was filtered and washed with ethyl acetate (3×5 ml). Solid was dried under reduced pressure to give **1** as off-white solid (0.14 g, 14.2%). Mp 245–247 °C; ^{1}H NMR (DMSO-d_6, 300 MHz): δ 3.19 (s, 3H, OCH_3), 6.15 (s, 1H, Ar), 7.03 (d, 2H, J = 8.4 Hz, Ar), 7.35 (broad s, 2H, NH_2), 7.90 (d, 2H, J = 8.4 Hz, Ar), 11.68 (s, 1H, Ar-OH); MS (ESI$^+$) m/z 218 (M+H)$^+$.

5.3.2. Preparation of 2-amino-6-(3,4-dimethoxyphenyl)pyrimidin-4-ol (2)

To a stirred solution of **25** (0.2 g, 0.79 mmol) and guanidine hydrochloride (0.11 g, 1.18 mmol) in ethanol (10 ml), potassium carbonate (0.16 g, 1.18 mmol) was added and refluxed for 48 h. Reaction mixture was cooled to rt, ethanol removed under vacuum, diluted with water (5 ml) and pH was adjusted to 6.5. The precip-

itated solid was filtered and washed with ethyl acetate (3 × 5 ml). Solid was dried under reduced pressure to give **2** as off-white solid (0.043 g, 22%). Mp 288–291 °C; ^{1}H NMR ($CDCl_3$, 300 MHz): δ 3.81 (s, 3H, OCH_3), 3.83 (s, 3H, OCH_3), 6.16 (s, 1H, Ar), 6.95 (broad s, 2H, NH_2), 7.01 (d, 1H, J = 8.4 Hz, Ar), 7.50 (s, 1H, Ar), 7.54 (dd, 1H, J = 4.5 and 8.4 Hz, Ar); MS (ESI$^+$) m/z 248 (M+H).

5.3.3. Preparation of 2-amino-6-(3,4-dimethoxyphenyl)pyrimidin-4-thiol (3)

To a suspension of **2** (0.15 g, 0.61 mmol) in toluene (5 ml) was added Lawesson's reagent (0.98 ml, 2.44 mmol) and heated at 110 °C for 8 h. Toluene was distilled out from the reaction mixture under vacuum and treated with ice (5 g) followed by sodium bicarbonate solution (5 ml). The resulting mixture was extracted with chloroform (2 × 50 ml) and washed with brine (2 × 20 ml). Solvent was removed under reduced pressure and crude compound was purified by silica gel column using methanol/chloroform as eluent. Solid dried under reduced pressure to give **3** as off-white solid (0.056 g, 35%). Mp 243–245 °C; ^{1}H NMR ($CDCl_3$, 300 MHz): δ 3.81 (s, 3H, OCH_3), 4.01 (s, 3H, OCH_3), 6.94 (broad s, 2H, NH_2), 7.01 (s, 1H, Ar), 7.03 (d, 1H, J = 8.4 Hz, Ar), 7.57 (d, 1H, J = 2.1 Hz, Ar), 7.65 (dd, 1H, J = 2.1 and 8.4 Hz, Ar); MS (ESI$^+$) m/z 264 (M+H)$^+$.

5.3.4. Preparation of 6-(4-methoxyphenyl)pyrimidine-2,4-diol (4)

The suspension of urea (500 mg, 8.32 mmol) in **25** (4 ml) was heated at 180–190 °C for 5–6 h. Reaction was monitored by TLC. Reaction mixture was cooled to rt, diluted with ethyl acetate (10 ml). The solid was filtered, washed with ethyl acetate (2 × 5 ml) to give **4** (437 mg, 24.06%). Mp 286–288 °C; ^{1}H NMR (DMSO-d_6, 300 MHz): δ 3.82 (s, 3H, OCH_3), 5.77 (s, 1H, Ar), 7.03 (d, 2H, J = 9.0 Hz, Ar), 7.70 (d, 2H, J = 9.0 Hz, Ar), 11.02 (s, 1H, Ar-OH), 11.07 (s, 1H, Ar-OH); MS (ESI$^+$) m/z 219 (M+H)$^+$.

5.3.5. Preparation of 2,4-dichloro-6-(4-methoxyphenyl)pyrimidine (1a)

The suspension of **4** (200 mg, 0.91 mmol) in $POCl_3$ (4 ml) was heated at 90 °C for 1 h. Reaction was monitored by TLC. After completion, excess $POCl_3$ was distilled off under vacuum. Ice and water were added to the residue, and the yellow product was filtered and washed with water till it reached neutral pH. Crude product was purified by silica gel column chromatography using chloroform as eluent to give **1a** (126.6 mg, 53.80%). Mp 103–105 °C; ^{1}H NMR ($CDCl_3$, 300 MHz): δ 3.91 (s, 3H, OCH_3), 7.03 (d, 2H, J = 9.0 Hz, Ar), 7.60 (s, 1H, Ar), 8.06 (d, 2H, J = 9.0 Hz, Ar); MS (ESI$^+$) m/z 255 (M+H)$^+$.

5.3.6. Preparation of 6-(4-methoxyphenyl)pyrimidine-2,4-diamine (1b)

In a sealed tube, suspension of **1a** (60 mg, 0.235 mmol) in liq. ammonia (9 ml) and ethanol (1 ml) was heated to 110 °C for 4–5 h. Reaction was monitored by TLC. Solvent was distilled off under vacuum to give crude product. Crude product was purified by silica gel column chromatography using methanol/chloroform as eluent to give **1b** (12 mg, 23.57%). Mp 210–212 °C; ^{1}H NMR (DMSO-d_6, 300 MHz): δ 3.82 (s, 3H, OCH_3), 6.20 (s, 1H, Ar), 6.55 (broad s, 2H, NH_2), 6.98 (broad s, 2H, NH_2), 7.04 d, 2H, J = 8.7 Hz, Ar), 7.81 (d, 2H, J = 8.7 Hz, Ar); MS (ESI$^+$) m/z 217 (M+H)$^+$.

5.3.7. Preparation of 4-chloro-6-(4-methoxyphenyl)pyrimidin-2-amine (26)

A stirred mixture of **1** (2.0 g, 9.21 mmol) and $POCl_3$ (50 ml) was heated to 120–125 °C for 2 h under dry nitrogen atmosphere. Once reaction mixture became clear, it was monitored by TLC for completion. After the completion of reaction, $POCl_3$ was distilled out under vacuum. Chloroform (100 ml) was added to crude mass and pH was adjusted to 6–7 by adding sodium bicarbonate solution. Organic layer was washed with brine solution (2 × 50 ml) and the solvent was distilled under vacuum to get crude product as yellow liquid oil. Crude compound was purified by silica gel column chromatography using methanol/chloroform as eluent to give **26** (1.65 g, 76.3%). Mp 201–203 °C; ^{1}H NMR (DMSO-d_6, 300 MHz): δ 3.82 (s, 3H, OCH_3), 7.01 (broad s, 2H, NH_2), 7.05 (d, 2H, J = 7.8 Hz, Ar), 7.19 (s, 1H, Ar), 8.06 (d, 2H, J = 7.8 Hz, Ar); MS (ESI$^+$) m/z 236 (M+H)$^+$.

5.3.8. Preparation of *N*-(2-amino-6-(4-methoxyphenyl)pyrimidin-4-yl) methanesulfonamide (1c)

A suspension of **26** (200 mg, 0.848 mmol), methane sulfonamide (161.4 mg, 1.69 mmol), potassium carbonate (234.4 mg, 1.69 mmol) in dimethyl sulfoxide (5 ml) was heated to 170 °C for 3–4 h. Reaction was monitored by TLC. The resulting mixture concentrated to dryness under reduced pressure. Cold water was added to reaction mixture and pH was neutralized to 6–7 by adding dil HCl solution. Crude product was filtered off and purified by silica gel column chromatography using methanol/chloroform eluent to give **1c** (82 mg, 32.8%). Mp 242–244 °C; ^{1}H NMR (acetone-d_6, 300 MHz): δ 3.33 (s, 3H, CH_3), 3.87 (s, 3H, OCH_3), 6.23 (broad s, H, NH_2), 6.78 (s, 1H, Ar), 7.01 (d, 2H, J = 8.1 Hz, Ar), 7.98 (d, 2H, J = 8.1 Hz, Ar); MS (ESI$^+$) m/z 295 (M+H)$^+$; HRMS calcd for $C_{12}H_{15}N_4O_3S$, 295.0859; found, 295.0848.

5.3.9. Preparation of 4-methoxy-6-(4-methoxyphenyl)pyrimidin-2-amine (1d)

Na metal (100 mg, 4.34 mmol) was dissolved in dry methanol (5 ml). **26** (100 mg, 4.24 mmol) was added and reaction mass was heated to reflux for 3–4 h. Reaction was monitored by TLC. Solvent was distilled under reduced pressure. Water was added to the reaction mixture and pH was adjusted to 6–7 by dil HCl solution. Product was filtered off and dried to give **1d** (62 mg, 63.26%). Mp 159–161 °C; ^{1}H NMR (DMSO-d_6, 300 MHz): δ 3.81 (s, 6H, OCH_3), 6.49 (s, 1H, Ar), 6.57 (broad s, 2H, NH_2), 7.04 (d, 2H, J = 5.4 Hz, Ar), 8.01 (d, 2H, J = 5.4 Hz, Ar); MS (ESI$^+$) m/z 231(M+H)$^+$.

5.4. High throughput in vitro assay

The assay was standardized based on previous protocols reported by Okamoto et al. and Sathisha et al.[21,30] Previous studies have reported uric acid absorption to be maximum at 290 nm which was reproduced by us on the Jasco spectrophotometer. Since the objective was to establish a high throughput assay, the assay was standardized using the Tecan system with the integrated Safire 2 reader. For this purpose, we used 96 well UV transparent plates from Corning Life Sciences, USA, instead of the quartz cuvettes used in the Jasco spectrophotometer. In this set up, the absorption peak of uric acid was found at 310 nm. At this wavelength a linearly increasing trend was observed for absorbance with increasing concentrations of uric acid. All further xanthine oxidase activity was monitored spectrophotometrically on the HTS system following the absorbance of uric acid at 310 nm under aerobic condition.

The XO activity was observed in presence of varied concentrations of bovine XO (Calbiochem) and xanthine (Sigma). The concentrations at which the formation of uric acid stabilized were found to be 200 mU XO and 400 μM xanthine at 30 min. These parameters were used for further screening. The enzyme solution of XO prepared in water was added to the test compounds or vehicle control (0.5% DMSO). The reaction was initiated by addition of xanthine in 50 mM potassium phosphate buffer (pH 7.5) as the substrate to the above assay mixture. The absorbance at 310 nm, indicating the formation of uric acid was measured at 30 min at ambient temperature. Duplicate assays were repeated three times. Allopurinol was used as positive control. The inhibitory activity of

each test compound against xanthine oxidase was indicated by their IC_{50} values.

5.5. In vivo efficacy

5.5.1. Animals

Six weeks old male Sprague–Dawley rats were obtained from central animal facility of Piramal Healthcare Ltd (formerly Piramal Life Sciences Limited, PLSL). The rats were acclimatized for one week to the laboratory environment. During this period, they were provided with water and normal pelleted diet (NPD) ad libitum. All the study protocols were approved by Institutional Animal Ethics Committee (IAEC) of PLSL, and performed in accordance with the guidelines of Committee for the Purpose of Control and Supervision on Experiments on Animals (CPCSEA), Government of India.

5.5.2. Potassium oxonate-induced hyperuricemic rat-model assay

Overnight fasted rats were grouped according to serum uric acid levels and were then treated with potassium oxonate (250 mg/kg) intraperitoneally to induce hyperuricemia. One hour after potassium oxonate administration, rats were treated with compounds **1** (100 mg/kg, po), **2** (50 mg/kg, ip), allopurinol (10 mg/kg, po), febuxostat (10 mg/kg, po) or vehicle (0.5% CMC). These doses were selected on the basis of literature and our previous experiments. About 250 μL of blood was collected from retro orbital plexus at 1, 2 and 4 h post drug treatment. Serum was obtained by allowing the blood sample to settle for 1 h at room temperature and centrifugation (Sigma 3K-30) at 4000 rpm for 20 min. Serum uric acid levels were measured photometrically (TBHBA method, Diasys kit) using an auto analyzer (Mindray BS400). Percent reduction in area under curve (AUC_{0-4h}) of the test compound was calculated by taking AUC_{0-4h} of the vehicle group as 100%.[18,41]

Acknowledgment

We are indebted to Dr. Somesh Sharma for his unstinting support for this structure-driven drug design project.

Supplementary data

Supplementary data associated with this article can be found, in the online version, at http://dx.doi.org/10.1016/j.bmc.2012.03.019. An animated Interactive 3D Complement (I3DC) is available in Proteopedia at http://proteopedia.org/w/Journal:BMC:3.

References and notes

1. Kim, K. Y.; Schumacher, R. H.; Hunsche, E.; Wertheimer, A. I.; Kong, S. X. *Clin. Ther.* **2003**, *25*, 1593.
2. Eggebeen, A. T. *Am. Fam. Physician* **2007**, *76*, 801.
3. Mapa, J. B.; Pillinger, M. H. *Curr. Opin. Invest. Drugs* **2010**, *11*, 499.
4. Adams, J. U. *Nat. Biotechnol.* **2009**, *27*, 309.
5. Terkeltaub, R. *Arthritis Res. Ther.* **2009**, *11*, 236.
6. Reinders, M. K.; Jansen, T. L. T. A. *Ther. Clin. Risk Manage.* **2010**, *6*, 543.
7. http://www.ardeabio.com/development-pipeline/gout.htm (last accessed on January 4, 2012).
8. http://www.drugs.com/clinical_trials/ardea-biosciences-announces-positive-results-rdea594-combination-febuxostat-allopurinol-gout-10558.html (last accessed on January 4, 2012).
9. Pacher, P.; Nivorozhkin, A.; Szabó, C. *Pharmacol. Rev.* **2006**, *58*, 87.
10. Hair, P. I.; McCormack, P. L.; Keating, G. M. *Drugs* **2008**, *68*, 1865.
11. Zhu, J. X.; Wang, Y.; Kong, L. D.; Yang, C.; Zhang, X. *J. Ethnopharmacol.* **2004**, *93*, 133.
12. Lin, C.-M.; Chen, C.-S.; Chen, C.-T.; Liang, Y.-C.; Lin, J.-K. *Biochem. Biophys. Res. Commun.* **2002**, *294*, 167.
13. Lewis, A. S.; Murphy, L.; Mccalla, C.; Fleary, M.; Purcell, S. *J. Biol. Chem.* **1984**, *259*, 12.
14. Liu, X.; Chen, R.; Shang, Y.; Jiao, B.; Huang, C. *Chem. Biol. Interact.* **2008**, *176*, 137.
15. Kumar, R.; Sharma, S.; Singh, R. *Expert Opin. Ther. Patents* **2011**, *21*, 1071.
16. Sato, T.; Ashizawa, N.; Iwanaga, T.; Nakamura, H.; Matsumoto, K.; Inoue, T.; Nagata, O. *Bioorg. Med. Chem. Lett.* **2009**, *19*, 184.
17. Sato, T.; Ashizawa, N.; Matsumoto, K.; Iwanaga, T.; Nakamura, H.; Inoue, T.; Nagata, O. *Bioorg. Med. Chem. Lett.* **2009**, *19*, 6225.
18. Ishibuchi, S.; Morimoto, H.; Oe, T.; Ikebe, T.; Inoue, H.; Fukunari, A.; Kamezawa, M.; Yamada, I.; Naka, Y. *Bioorg. Med. Chem. Lett.* **2001**, *11*, 879.
19. Fukunari, A.; Okamoto, K.; Nishino, T.; Eger, B. T.; Pai, E. F.; Kamezawa, M.; Yamada, I.; Kato, N. *J. Pharmacol. Exp. Ther.* **2004**, *311*, 519.
20. Wang, S.; Yan, J.; Wang, J.; Chen, J.; Zhang, T.; Zhao, Y.; Xue, M. *Eur. J. Med. Chem.* **2010**, *45*, 2663.
21. Sathisha, K. R.; Khanum, S. A.; Chandra, J. N. N. S.; Ayisha, F.; Balaji, S.; Marathe, G. K.; Gopal, S.; Rangappa, K. S. *Bioorg. Med. Chem.* **2011**, *19*, 211.
22. Niu, Y.; Zhu, H.; Liu, J.; Fan, H.; Sun, L.; Lu, W.; Liu, X.; Li, L. *Chem. Biol. Interact.* **2011**, *189*, 161.
23. Oettl, K.; Reibnegger, G. *Biochim. Biophys. Acta* **1999**, *1430*, 387.
24. Hsieh, J.-F.; Wu, S.-H.; Yang, Y.-L.; Choong, K.-F.; Chen, S.-T. *Bioorg. Med. Chem.* **2007**, *15*, 3450.
25. Masuoka, N.; Kubo, I. *Biochim. Biophys. Acta* **2004**, *1688*, 245.
26. Shen, L. Ji, H.-fang *Bioorg. Med. Chem. Lett.* **2009**, *19*, 5990.
27. Nepali, K.; Agarwal, A.; Sapra, S.; Mittal, V.; Kumar, R.; Banerjee, U. C.; Gupta, M. K.; Satti, N. K.; Suri, O. P.; Dhar, K. L. *Bioorg. Med. Chem.* **2011**, *19*, 5569.
28. Nepali, K.; Singh, G.; Turan, A.; Agarwal, A.; Sapra, S.; Kumar, R. *Bioorg. Med. Chem.* **2011**, *19*, 1950.
29. Truglio, J. J.; Theis, K.; Leimkuhler, S.; Rappa, R.; Rajagopalan, K. V.; Kisker, C. *Structure* **2002**, *10*, 115.
30. Okamoto, K.; Eger, B. T.; Nishino, T.; Kondo, S.; Pai, E. F.; Nishino, T. *J. Biol. Chem.* **2003**, *278*, 1848.
31. Okamoto, K.; Matsumoto, K.; Hille, R.; Eger, B. T.; Pai, E. F.; Nishino, T. *Proc. Natl. Acad. Sci. U.S.A.* **2004**, *101*, 7931.
32. Enroth, C.; Eger, B. T.; Okamoto, K.; Nishino, T.; Nishino, T.; Pai, E. F. *Proc. Natl. Acad. Sci. U.S.A.* **2000**, *97*, 10723.
33. Pauff, J. M.; Cao, H.; Hille, R. *J. Biol. Chem.* **2009**, *284*, 8760.
34. Okamoto, K.; Nishino, T. *J. Biol. Chem.* **1995**, *270*, 7816.
35. Lagunin, A.; Stepanchikova, A.; Filimonov, D.; Poroikov, V. *Bioinformatics* **2000**, *16*, 747.
36. GLIDE, *version 5.6*; Schrödinger, LLC: New York, NY, 2010.
37. *The PyMOL Molecular Graphics System, Version 1.2r2*; Schrödinger, LLC.
38. Jaffe, I. A. *Am. J. Med.* **1986**, *80*, 471.
39. Seidler, J.; Mcgovern, S. L.; Doman, T. N.; Shoichet, B. K. *Drugs* **2003**, *46*, 4477.
40. Friesner, R. A.; Murphy, R. B.; Repasky, M. P.; Frye, L. L.; Greenwood, J. R.; Halgren, T. A.; Sanschagrin, P. C.; Mainz, D. T. *J. Med. Chem.* **2006**, *49*, 6177.
41. Osada, Y.; Tsuchimoto, M.; Fukushima, H.; Takahashi, K.; Kondo, S.; Hasegawa, M.; Komoriya, K. *Eur. J. Pharmacol.* **1993**, *241*, 183.